Fragility functions for performance-based ground failure due to soil liquefaction

Brett W. Maurer
Department of Civil & Environmental Engineering – University of Washington, Seattle, WA, USA
Sjoerd van Ballegooy
Tonkin + Taylor Ltd, Auckland, New Zealand
Brendon A. Bradley
Department of Civil & Natural Resources Engineering – University of Canterbury, Christchurch, New Zealand

ABSTRACT
The severity of liquefaction manifested at the ground surface is a pragmatic proxy of damage potential for various infrastructure assets, making it particularly useful for hazard mapping, land-use planning, and preliminary site-assessment. Towards this end, the recent Canterbury, New Zealand, earthquakes, in conjunction with others, have resulted in liquefaction case-history data of unprecedented quantity and quality, presenting a unique opportunity to rigorously develop fragility-functions for liquefaction-induced ground failure. Accordingly, this study analyzes nearly 10,000 liquefaction case studies from 23 global earthquakes to develop fragility functions for use in performance-based frameworks. The proposed functions express the probability of exceeding specific severities of liquefaction surface manifestation as a function of three different liquefaction damage measures (*LDMs*), wherein four alternative liquefaction-triggering models are used. These functions have the same functional form, such that end-users can easily select the model coefficients for the particular damage state, triggering model, and *LDM* of their choosing. It should be noted that these functions are not to be used to predict lateral spreading, which requires *LDMs* other than those assessed herein. Lastly, the proposed functions are preliminary and subject to further development. In this regard, several thrusts of ongoing investigation are discussed.

1 INTRODUCTION

In performance-based earthquake engineering, fragility-functions relate the probability of an undesirable outcome (e.g., the ground exceeding a defined state of damage) to a particular measure of excitation or demand. In the case of performance-based damage assessment of soil liquefaction, the severity of liquefaction manifested at the ground surface can be used as a pragmatic proxy of damage potential for various infrastructure assets, making it particularly useful for hazard mapping, land-use planning, and preliminary site-assessment.

Towards this end, the development of empirical fragility-functions for predicting manifestation severity relies on high-quality liquefaction case-history data. However, due to the cost and difficulty of obtaining this data, only about 300 well-documented cases had been assembled from all combined earthquakes occurring prior to 2010. The potential for compiling such data was then dramatically increased, both in quantity and in quality, following the 2010-2016 Canterbury, New Zealand, Earthquake Sequence (CES), which induced widespread and severe liquefaction in the city of Christchurch. In conjunction with existing case histories, the CES presents a truly unique opportunity to rigorously develop and assess fragility functions for liquefaction-induced ground failure. Accordingly, this study analyzes 265 case histories from 20 global earthquakes and 9,623 case histories from three CES earthquakes to develop fragility functions for performance-based frameworks. These functions express the probability of exceeding specific severities of liquefaction surface manifestation as a function of three different liquefaction damage measures (*LDMs*), wherein four alternative liquefaction-triggering models are used. Specifically, this study investigates the probabilistic relationship between the severity of liquefaction surface manifestation and the following *LDMs:* (1) the liquefaction potential index (*LPI*) (Iwasaki et al. (1978); (2) a modified LPI, termed LPI_{ISH} (Maurer et al., 2015a); and (3) the liquefaction severity number (*LSN*) (Van Ballegooy et al., 2014a). The developed functions have the same functional form, such that end-users can easily select the model coefficients for the particular damage state, triggering model, and *LDM* of their choosing.

2.0 DATA

This study analyzes 9,908 liquefaction case histories resulting from 23 global earthquakes, as summarized in Table 1. However, because the majority of these cases were compiled from three events during the CES, results are separately presented for these and the other 20 earthquakes, henceforth respectively referred to as the "CES dataset" and "global dataset." These datasets are discussed subsequently, followed by a summary of the methods used to analyze them.

2.1 Canterbury Earthquakes Sequence (CES) Dataset

The CES resulted in case-history data of unprecedented quantity and quality, presenting a unique opportunity to advance the science of liquefaction hazard assessment. A summary of the CES, to include tectonic and geologic settings, seismology, and environmental effects, is

provided by Quigley et al. (2016). The present study uses data from the M_w7.1, 4 Sept. 2010 Darfield earthquake, the M_w6.2, 22 Feb. 2011 Christchurch earthquake, and the M_w5.7, 14 Feb. 2016 Christchurch earthquake. Ground motions from these events were recorded by a dense network of strong motion stations (e.g., Bradley and Cubrinovski, 2011) and due to the impacts of liquefaction, the New Zealand Earthquake Commission funded an extensive geotechnical reconnaissance and testing program (Tonkin + Taylor, 2013) that included ground water modeling and in-situ and laboratory soil testing. The combination of densely recorded ground motions, well-documented liquefaction response, and detailed subsurface characterization comprises the CES dataset. These data are succinctly summarized as follows.

Table 1. Summary of liquefaction case histories analyzed

Date	Event	Country	M_w	# Cases
16/6/1964	Niigata	Japan	7.60	3
9/2/1971	San Fernando	USA	6.60	2
4/2/1975	Haicheng	China	7.00	2
27/7/1976	Tangshan	China	7.60	10
15/10/1979	Imperial Valley	USA	6.53	5
9/6/1980	Victora (Mexicali)	Mexico	6.33	5
26/4/1981	Westmoreland	USA	5.90	7
26/5/1983	Nihonkai-Chubu	Japan	7.70	2
28/10/1983	Borah Peak	USA	6.88	3
2/3/1987	Edgecumbe	NZ	6.60	23
24/11/1987	Superstition Hills	USA	6.54	8
18/10/1989	Loma Prieta	USA	6.93	61
17/1/1994	Northridge	USA	6.69	3
16/1/1995	Hyogoken-Nambu	Japan	6.90	21
17/8/1999	Kocaeli	Turkey	7.51	16
20/9/1999	Chi-Chi	Taiwan	7.62	37
8/6/2008	Achaia-Ilia	Greece	6.40	2
4/4/2010	El Mayor-Cucapah	Mexico	7.20	2
4/10/2010	Darfield	NZ	7.10	3647
22/2/2011	Christchurch	NZ	6.20	3700
11/3/2011	Tohoku	Japan	9.00	7
20/5/2012	Emilia	Italy	6.10	46
14/2/2016	Christchurch	NZ	5.70	2296
			Total	9908

2.1.1 CPT Soundings

Drawing from a subset of data available in the New Zealand Geotechnical Database (NZGD, 2016), this study utilizes 3,834 CPT soundings performed at sites where the severity of liquefaction manifestation was documented following the Sept 2010 Darfield, Feb 2011 Christchurch, and/or Feb 2016 Christchurch earthquakes, resulting in a combined 10,881 case histories. In the process of compiling these cases, CPTs were first rejected if: (1) performed at sites where the predominant manifestation of liquefaction was lateral spreading; (2) the depth of "pre-drill" exceeded the depth of the ground water table; and (3) inferred to have prematurely terminated on shallow gravels using a geospatial autocorrelation analysis (Anselin, 1995), which identifies spatial outliers. Extended coverage of CPT data and the exclusion criteria summarized above is provided in Maurer et al. (2014, 2015b).

2.1.2 Peak Ground Acceleration (PGA)

Peak Ground Accelerations (PGAs) at the ground surface were computed with the Bradley (2013) procedure, which has been used by many CES studies (e.g., Green et al. 2014; Maurer et al., 2015c; van Ballegooy et al. 2015). This procedure geostatistically coalesces estimates from ground-motion prediction equations with strong-motion recordings.. In addition to the exclusion criteria described in the section above, cases with PGA < 0.15g were removed from the dataset. This criterion was applied because sites with PGAs below a certain threshold have negligible probability of liquefaction, and thus, do not provide meaningful inputs for assessing the probability of manifestations. In particular, 0.15g was selected because no site experiencing a PGA below this threshold had manifestations in any CES event. Research is ongoing to further develop this criterion. Following the removal of cases with PGA < 0.15g, a total of 9,623 cases remain.

2.1.3 Ground Water Table (GWT) Depth

For this study, GWT depths were sourced from the robust, event-specific regional ground water models of van Ballegooy et al. (2014b). These models, which reflect seasonal and localized fluctuations across the region, were derived in part using monitoring data from a network of ~1000 piezometers and provide a best-estimate of GWT depths immediately prior to each earthquake.

2.1.4 Liquefaction Severity

Observations of liquefaction and the severity of surface manifestation (extent and severity of liquefaction ejecta) were made by the authors for each CPT location following each of the three aforementioned earthquakes. The severity of manifestation was classified using criteria similar to Green et al. (2014), such that manifestations are ranked as "none," "minor," "moderate," or "severe." Of the 9,623 cases compiled from the CES, 60% are "none" and 40% are cases where manifestations were observed and classified (22% minor; 15% moderate; 3% severe).

Table 2. Manifestation severity ranking-criteria.

Classification	Criteria
No Manifestation	No manifestation or lateral spread cracking
Minor Manifestation	Small, isolated liquefaction features; streets had traces of ejecta less than a vehicle width; < 5% of ground surface covered by ejecta
Moderate Manifestation	Groups of features; streets had ejecta patches greater than a vehicle width but were passable; 5-40% of ground surface covered by ejecta
Severe Manifestation	Masses of adjoining features; >40% of ground surface covered by ejecta; streets impassible

Figure 1. Representative observations of three classes of manifestation severity: (a) marginal; (b) moderate; and (c) severe, in accordance with the Green et al. (2014) criteria.

2.2 Global Dataset

To compare performance findings in Christchurch with regions worldwide, 265 liquefaction case histories resulting from 20 global earthquakes in nine countries are compiled and assessed in parallel. These case histories are sourced from the existing literature, to include CPT sounding data, observations of manifestation severity, and estimation of GWT depth and PGA, as generally reported by original investigators. When possible, recent refinements of PGA and/or GWT depth are adopted from the literature. To properly recognize all sources of data used to compile the global dataset, a reference list appears in the Appendix for each of the 20 earthquakes. The case history assemblages of Moss et al. (2005) and Boulanger and Idriss (2014) are also acknowledged for greatly assisting the present study. In compiling these 265 cases, those with PGA < 0.15g were removed for consistency with the CES dataset. Notably, the CES and global datasets deviate in the classification of manifestation severity. Whereas CES liquefaction was intensively cataloged via reconnaissance and remote sensing, the global cases are often insufficiently documented for manifestations to be classified in the same level of detail. In the present study, surficial manifestations are therefore classified binomially as “yes” or “no” without categorizing the nature or severity of expression. Of the 265 cases compiled, 39% are “no” and 61% are “yes.”

3.0 METHODOLOGY

3.1 Liquefaction Triggering Models & Damage Measures

In current practice, several alternative liquefaction-triggering models and several different *LDMs* are commonly used. While regional codes sometimes mandate use of a particular methodology, there is no professional consensus on which is best. Accordingly, the proposed research will use an array of triggering models and *LDMs*, such that end-users can utilize the specific combination of their choosing. In particular, this study will investigate the relationship between manifestation severity, as classified herein, and each of the following *LDMs*: (1) the liquefaction potential index (*LPI*), as defined by Iwasaki et al. (1978); (2) a modified *LPI*, termed LPI_{ISH} (Maurer et al., 2015a); and (3) the liquefaction severity number (*LSN*) proposed by Van Ballegooy et al. (2014a).

Intrinsic to each of the above *LDMs*, the safety factor against liquefaction triggering (FS_{liq}) is computed from a liquefaction-triggering model. For this study, FS_{liq} values will be separately computed by the deterministic Robertson and Wride (1998)[RW98], Moss et al. (2006)[Mea06], Idriss and Boulanger (2008)[IB08], and Boulanger and Idriss (2014)[BI14] models. Antecedent to using these models, soils susceptible to liquefaction will be identified using the soil-behavior-type-index (I_c) proposed by Robertson and Wride (1998) such that soils with $I_c < 2.50$ are treated as susceptible. This criterion was developed specifically for Christchurch soils from lab tests on more than 2,000 samples (Maurer et al., 2016). However, because an I_c threshold of 2.50 is within the range of values commonly used in practice, this criterion is also applied in all analyses of the global dataset. For liquefaction-susceptible soils, the IB08 and BI14 procedures compute liquefaction resistance as a function of fines-content (*FC*). Accordingly, *FC* is estimated for the CES dataset using a Christchurch-specific I_c – *FC* correlation (Maurer et al., 2016), and for the global dataset using a general I_c – *FC* correlation (Boulanger and Idriss, 2014).

3.2 Fragility Functions

The probability of the surface manifestation of liquefaction reaching or exceeding a manifestation severity, *MS*, given a computed *LDM* value, is herein denoted $F_{MS}(LDM)$ and idealized by a lognormal distribution, as is typical for fragility functions (e.g., Bradley, 2010):

$$F_{MS}(LDM) = \Phi\left(\frac{\ln(\frac{LDM}{x_m})}{\beta}\right) \quad [1]$$

where Φ denotes the Gaussian cumulative distribution function; x_m is the distribution median, and β is the logarithmic standard deviation. While several approaches exist for fitting functions to data, this study utilizes the maximum likelihood method described in Porter (2016), which identifies the model parameters with the highest likelihood of producing the observed data. Specifically, the case histories are grouped into m bins of similar *LDM*, where bins have index i, average value LDM_i, and contain n_i cases, of which f_i are cases in which observed manifestations reached or exceeded *MS*. Assuming quantity f_i can be estimated from a binomially-distributed random variable, F_i, Eq. 2 gives the probability of observing quantity f_i among n_i cases, if the probability of an individual case exceeding *MS* is given by Eq. 1.

$$P[F_i = f_i] = \frac{n_i!}{f_i!(n_i - f_i)!} \cdot p_i{}^{f_i} \cdot (1 - p_i)^{n_i - f_i} \quad [2]$$

In Eq. 2, p_i is defined by Eq. 1, evaluated at LDM_i. Lastly, the values of parameters x_m and β that maximize the likelihood of producing the observed data are determined. This likelihood is given by the product of the probabilities in Eq. 2, multiplied over all bins:

$$L\,(X_m, \beta) = \prod_{i=1}^{m} P[F_i = f_i] \quad [3]$$

4.0 RESULTS AND DISCUSSION

Using the approach outlined above and analyses of nearly 10,000 liquefaction case studies, fragility functions were developed as functions of *LPI*, LPI_{ISH}, and *LSN* values, which were each separately computed using the RW98, Mea06, IB08, and BI14 liquefaction triggering models. The developed functions are all of the form presented in Eq. 1, such that end-users can easily select the x_m and β values for the particular manifestation-severity, triggering model, and *LDM* of their choosing. As an example, the suite of functions developed for use with *LPI* and the RW98 model is plotted in Fig. 2. As previously discussed, the CES and global datasets deviate in the classification of manifestation severity, such that manifestations in the latter dataset are classified binomially as "yes" or "no." Consequently, analyses of the global dataset result in one fragility-function for "unclassified manifestations," whereas analyses of the CES dataset result in fragility-functions for "minor," "moderate," and "severe" manifestations.

As shown in Fig. 2, the developed functions relate the probability of reaching or exceeding a manifestation severity, *MSi*, to a computed *LDM* value (in this case, *LPI*). As an example, the probabilities of manifestations being *at least* minor, moderate, and severe at *LPI* = 5 are 57%, 23%, and 1%, respectively. For the global dataset, the probability of observing *any* manifestation at *LPI* = 5 is approximately 54%. In this regard, results from the CES and global datasets are very similar (i.e., 57% vs. 54%). The developed functions can also assess the probability that manifestations will be *in* a particular severity class. This is illustrated in Fig. 2, where P0, P1, P2, and P3 are the respective probabilities that *MS* will be none, minor, moderate, and severe. In Fig. 3, these probabilities are plotted for all *LPI* values from the CES. Again using *LPI* = 5 as an example, the probabilities of manifestations being none, minor, moderate, and severe are 43%, 34%, 22%, and 1%, respectively. A summary of all fragility-functions is provided in Table 3, from which users can select the values of x_m and β corresponding to the particular manifestation severity, triggering model, and *LDM* of their choosing. In addition, the parameter-space of the *LDM* data is also provided for each function. Discretion is advised when using the functions beyond these recommended limits.

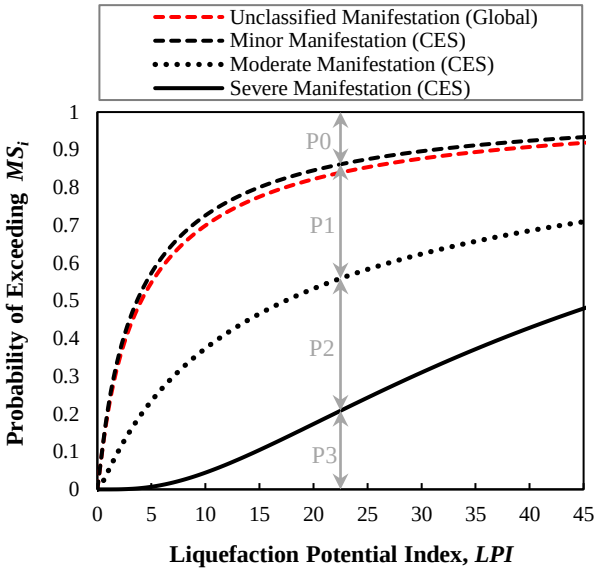

Figure 2. The probability of *exceeding* manifestation severity, MS_i, given an *LPI* value computed using the RW98 model. For the CES dataset, P0, P1, P2, and P3 are the respective probabilities that manifestation severity is none, minor, moderate, and severe.

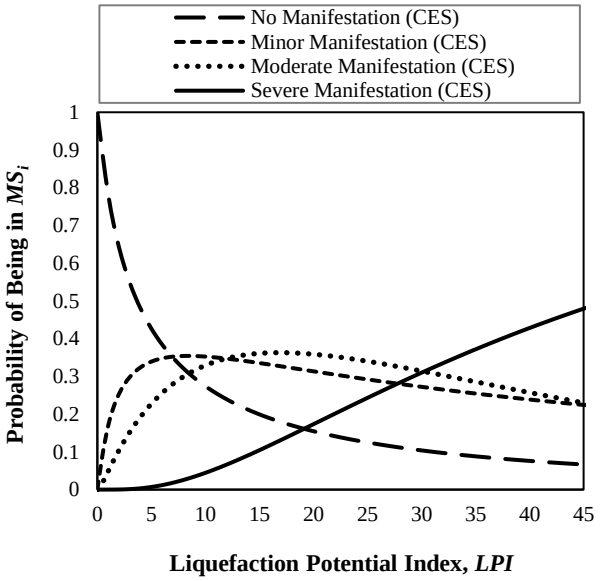

Figure 3. The probability of manifestations being *in* a severity class, MS_i, given an *LPI* computed using RW98.3

Table 3. Summary of fragility-functions developed for an array of *LDMs* and triggering models.

Dataset	Triggering Model	Manifestation Severity	LPI			LPI_{ISH}			LSN		
			x_m	β	Parameter Space	x_m	β	Parameter Space	x_m	β	Parameter Space
CES	RW98	Minor	3.672	1.667	LPI ≤ 50	1.766	2.249	LPI_{ISH} ≤ 43	12.836	1.747	LSN ≤ 68
		Moderate	17.420	1.722		13.955	2.349		49.495	1.584	
		Severe	47.172	0.912		86.710	1.814		202.900	1.335	
	Mea06	Minor	4.984	1.678	LPI ≤ 46	3.764	1.937	LPI_{ISH} ≤ 49	20.327	2.467	LSN ≤ 79
		Moderate	23.140	2.041		21.427	2.185		126.924	2.543	
		Severe	65.414	1.151		188.146	2.149		561.312	1.825	
	IB08	Minor	2.393	1.756	LPI ≤ 43	1.372	2.091	LPI_{ISH} ≤ 41	9.231	1.976	LSN ≤ 60
		Moderate	12.583	1.897		11.234	2.802		41.922	1.819	
		Severe	46.167	1.091		112.449	2.210		229.000	1.588	
	BI14	Minor	6.261	1.059	LPI ≤ 58	3.972	1.292	LPI_{ISH} ≤ 52	15.910	1.131	LSN ≤ 65
		Moderate	18.978	1.154		14.278	1.417		39.889	1.164	
		Severe	56.719	0.827		53.983	1.036		198.626	1.304	
Global	RW98	Unclassified Manifestation	4.061	1.726	LPI ≤ 56	0.668	3.715	LPI_{ISH} ≤ 47	8.167	1.538	LSN ≤ 67
	Mea06		4.852	1.581	LPI ≤ 52	2.242	2.299	LPI_{ISH} ≤ 42	11.551	1.456	LSN ≤ 80
	IB08		6.773	1.290	LPI ≤ 63	3.673	1.958	LPI_{ISH} ≤ 54	14.326	1.230	LSN ≤ 85
	BI14		3.101	2.280	LPI ≤ 56	1.177	3.190	LPI_{ISH} ≤ 49	8.314	1.113	LSN ≤ 61

4.1 Thrusts of Ongoing Investigation

The fragility-functions summarized in Table 3 are preliminary and subject to further development. In this regard, several thrusts of ongoing investigation are briefly summarized as follows:

- At present, PGAs have been estimated using empirical ground motion prediction equations (GMPEs) statistically coalesced with strong-motion recordings. However, this approach can be inaccurate when local phenomena are not captured by GMPEs. In contrast, physics-based simulations can provide significant insight into such phenomena, to include the effects of rupture directivity, basin-generated surface waves, and near-surface stratigraphic and topographic features. Physics-based simulations are being developed for CES events and have been shown to predict recorded motions better than GMPEs. Accordingly, PGAs will be updated for each CES case-study utilizing ground-motion simulations.
- At present, fragility-function uncertainties have not been considered. While the proposed functions predict the probability of being *in* a given damage state, the uncertainty therein is also of interest and will be accounted for in the future. Moreover, aleatoric and epistemic uncertainties will be separately considered, quantified, and propagated.
- The CES and global datasets are under ongoing development. In particular, it is anticipated that an additional 4,000 CES cases will soon be compiled, such that cases coincide with locations where presently collected CPT data is scarce. In addition, an attempt will be made to categorize the severity of manifestations for the historic global dataset (i.e., to improve upon the current binomial classification).
- Analyses will be undertaken to determine whether results derived from the CES are applicable worldwide. It is hypothesized that fragility-curves for the global "unclassified manifestations" should plot between the CES "marginal" and "moderate" manifestation fragility-curves. This is based on the assumption that the threshold for classifying historic cases as "yes" (i.e., some manifestation) lies in between the Green et al. (2014) criteria for "minor" and "moderate" manifestations. Notably, the functions with lowest dispersion, for both the CES and global datasets, are those developed for use with BI14. However, whereas BI14 used with LPI has the lowest β for the CES data, BI14 used with LSN has the lowest β for the global data.
- Fragility-functions are commonly assumed to have a lognormal distribution. However, the Lilliefors (1967) test will be used to assess whether this distribution is appropriate. In either case, there are many alternative approaches for fitting fragility functions to data (e.g., Baker, 2015) and several will be investigated.
- To use the proposed fragility-functions, the *LDMs* and triggering-functions must be employed exactly as used herein (detailed in sections 2.1.1 through 3.1). Most

notably, the proposed functions can only be used in conjunction with the *deterministic* liquefaction triggering-models of RW98, Mea06, IB08, and BI14. In the future, the fragility-functions will be updated to be compatible with analyses that also consider model and measurement uncertainties.

5.0 CONCLUSION

This study analyzed nearly 10,000 liquefaction case histories from 23 global earthquakes to develop fragility functions for use in performance-based frameworks. The proposed functions express the probability of exceeding well-defined severities of liquefaction surface manifestation as a function of three different liquefaction damage measures (*LDMs*), wherein four alternative liquefaction-triggering models are used. These functions have the same functional form, such that end-users can easily select the model coefficients for the particular manifestation severity, triggering model, and *LDM* of their choosing. These functions are preliminary and subject to further development. In this regard, several thrusts of ongoing investigation were discussed.

5.1 Acknowledgements

The authors express their gratitude to Professor Steven L. Kramer of the University of Washington for providing review comments that greatly improved this paper.

6.0 APPENDIX

The sources of data used in the compilation of the global dataset are listed as follows, parsed by event: **1964 M_w7.6 Niigata, JPN** - Ishihara and Koga (1981), Farrar (1990), Moss et al. (2003); **1971 M_w6.6 San Fernando, USA -** Bennett et al., 1998, Toprak and Holzer (2003); **1975 M_w7.0 Haicheng, CHN -** Arulandan et al. (1986), Shengcong and Tatsuoka (1984); **1976 M_w7.6 Tangshan, CHN -** Shibata and Teparaska (1988), Moss et al. (2009; 2011); **1979 M_w6.53 Imperial Valley, USA** - Diaz-Rodriguez (1984), Diaz-Rodriguez and Armijo-Palaio (1991), Moss et al. (2003); **1981 M_w5.9 Westmoreland, USA** - Bennett et al. (1984), Seed et al. (1984), Cetin et al. (2000), Moss et al. (2005); **1983 M_w7.7 Nihonkai-Chubu, JPN** - Farrar (1990); **1983 M_w6.88 Borah Peak, USA -** Andrus (1986), Andrus & Youd (1987), Moss et al. (2003); **1987 M_w6.6 Edgecumbe, NZ** - Christensen (1995), Moss et al. (2003); **1987 M_w6.54 Superstition Hills, USA** - Bennett et al. (1984), Cetin et al. (2000), Toprak and Holzer (2003), Moss et al. (2005), Holzer and Youd (2007); **1989 M_w6.93 Loma Prieta, USA** - Mitchell et al. (1994), Pass (1994), Bennett & Tinsely (1995), Boulanger et al. (1995; 1997), Kayen et al. (1998), Toprak & Holzer (2003), Youd and Carter (2005); **1994 M_w6.69 Northridge, USA** - Abdel-Haq & Hryciw (1998), Bennett et al., 1998, Holzer et al. (1999), Moss et al. (2003); **1995 M_w6.9 Hyogoken-Nambu, JPN** - Suzuki et al. (2003); **1999 M_w7.51 Kocaeli, TUR -** PEER (2000a), Youd et al. (2009); **1999 M_w7.62 Chi-Chi, TWN** - Lee et al. (2000), PEER (2000b); **2008 M_w6.4 Achaia-Ilia, GRC** - Batilas et al. (2014); **2008 M_w7.2 El Mayor-Cucapah, MEX** - Moss et al. (2005); CESMD (2016), Turner et al. (2016); **2011 M_w9 Tohoku, JPN** - Cox et al. (2013), Boulanger and Idriss (2014); **2012 M_w6.1 Emilia, ITA** - Papathanassiou et al. (2015), Facciorusso et al. (2015), Servizio Geologico (2016).

7.0 REFERENCES

Abdel-Haq, A., and Hryciw, R. D. 1998. Ground settlement in Simi Valley following the Northridge earthquake. *Journal of Geotechnical and Geoenvironmental*, 124(1): 80-89.

Andrus, R.D. 1986. Subsurface investigations on a liquefaction induced lateral spread Thousand Springs Valley, Idaho: liquefaction recurrence and a case history in gravel. M.S. Thesis, Dept. of Civil Engineering, Brigham Young University, Provo, Utah.

Andrus, R. D. and Youd, T. L. 1987. Subsurface Investigation of a Liquefaction-Induced Lateral Spread Thousand Springs Valley, Idaho. Misc. paper GL-87-8, U.S. Army Corps of Engineers.

Anselin, L. 1995. Local Indicators of Spatial Association—LISA. *Geographical Analysis*, 27(2): 93–115.

Arulanandan, K., Yogachandran, C., Meegoda, N. J., Ying, L., and Zhauji, S. 1986. Comparison of the SPT, CPT, SV and electrical methods of evaluating earthquake induced liquefaction susceptibility in Ying Kou City during the Haicheng Earthquake. Use of in situ tests in geotechnical engineering." Geotech. Spec. Publ., 6, 389–415.

Batilas, A., Pelekis, P., Vlachakis, V., and Athanasopoulos, G. 2014. Soil Liquefaction/Nonliquefaction in the Achaia-Ilia (Greece) 2008 Earthquake: Field Evidence, Site Characterization and Ground Motion Assessment. *International Journal of Geoengineering Case histories*, 2(4): 270-287.

Bennett, M. J., McLaughlin, P. V., Sarmiento, J. S., and Youd, T. L. 1984. Geotechnical investigation of liquefaction sites, Imperial Valley, California. U.S. Geological Survey, Open-File Report 84-252, 103 pp.

Bennett, M. J., Ponti, D. J., Tinsley, J. C., III, Holzer, T. L., and Conaway, C. H. 1998. Subsurface geotechnical investigations near sites of ground deformations caused by the January 17, 1994, Northridge, California, earthquake. U.S. Geological Survey, Open-file report 98-373, 148 pp.

Bennett, M. J., and Tinsley, J. C., III 1995. 'Geotechnical data from surface and subsurface samples outside of and within liquefaction-related ground failures caused by the October 17, 1989, Loma Prieta earthquake, Santa Cruz and Monterey Counties, California.' U.S. Geological Survey Open-File Rep. 95-663, U.S. Geological Survey.

Boulanger, R. W., Idriss, I. M., and Mejia, L. H. 1995. Investigation and evaluation of liquefaction related ground displacements at Moss Landing during the 1989 Loma Prieta earthquake. Report No. UCD/CGM-95/02, Center for Geotechnical Modeling, Department of Civil & Environmental Engineering, University of California, Davis, 231 pp., May.

Boulanger, R. W., Mejia, L. H., and Idriss, I. M. 1997.

Liquefaction at Moss Landing during Loma Prieta earthquake. *Journal of Geotechnical and Geoenvironmental Engineering,* 123(5): 453–67.

Boulanger, R.W. and Idriss, I.M. 2014. CPT and SPT based liquefaction triggering procedures. *Report No. UCD/CGM.-14/01*, Center for Geotech. Modelling, Department of Civil and Environmental Engineering, UC Davis, CA, USA.

Bradley, B.A. 2010. Epistemic uncertainties in component fragility functions. *Earthquake Spectra*, 26(1): 41-62.

Bradley, B.A. & Cubrinovski, M. 2011. Near-source Strong Ground Motions Observed in the 22 February 2011 Christchurch Earthquake. *Seismological Research Letters*, 82, 853-865.

Bradley, B.A. 2013. Site-specific and spatially-distributed ground motion intensity estimation in the 2010-2011 Christchurch earthquakes. *Soil Dynamics and Earthquake Engineering*, 48, 35-47.

CESMD 2016. U.S. structural and ground response data. Center for Engineering Strong Motion Data; http://www.strongmotioncenter.org/

Cetin, K. O., Seed, R. B., Moss, R. E. S., Der Kiureghian, A. K., Tokimatsu, K., Harder, L. F., and Kayen, R. E. 2000. Field Performance Case Histories for SPT-Based Evaluation of Soil Liquefaction Triggering Hazard. Geotechnical Engineering Research Report No. UCB/GT-2000/09, Geotechnical Engineering, Department of Civil Engineering, UC Berkeley.

Christensen, S. A. 1995. Liquefaction of Cohesionless Soils in the March 2, 1987 Edgecumbe Earthquake, Bay of Plenty, New Zealand, and Other Earthquakes. Masters of Engineering Thesis, Department of Civil Engineering, University of Canterbury, Christchurch, New Zealand.

Cox, B. R., Boulanger, R. W., Tokimatsu, K., Wood, C., Abe, A., Ashford, S., Donahue, J., Ishihara, K., Kayen, R., Katsumata, K., Kishida, T., Kokusho, T., Mason, B., Moss, R., Stewart, J., Tohyama, K., and Zekkos, D. 2013. Liquefaction at strong motion stations and in Urayasu City during the 2011 Tohoku-Oki earthquake." *Earthquake Spectra*, 29(S1): S55-S80.

Diaz-Rodriquez, J. A. 1984. Liquefaction in the Mexicali Valley During the Earthquake of June 9, 1980. Eighth World Conference on Earthquake Engineering EERI, San Francisco, 223-230.

Diaz-Rodriquez, J. A., and Armijo-Palacio, G. 1991. Liquefaction potential of fine cohesionless soils using the CPT. *Soils and Foundations*, 31(3): 111-119.

Facciorusso, J., Madiai, C., and Vannucchi, G. 2015. CPT-Based Liquefaction Case History from the 2012 Emilia Earthquake in Italy. *Journal of Geotechnical and Geoenvironmental Engineering,* 141(12): 05015002.

Farrar, J. A. 1990. Study of In Situ Testing for Evaluation of Liquefaction Resistance. R-90-06, U.S. Department of the Interior, Bureau of Reclamation, Research and Laboratory Services Division, Geotechnical Services Branch, Denver Office.

Green, R.A., Cubrinovski, M., Cox, B., Wood, C., Wotherspoon, L., Bradley, B., & Maurer, B.W. 2014. Select Liquefaction Case Histories from the 2010-2011 Canterbury Earthquake Sequence. *Earthquake Spectra*, 30(1), 131-153.

Holzer, T.L and Youd, T.L. 2007. Liquefaction, Ground Oscillation, and Soil Deformation at the Wildlife Array. *Bulletin of the Seismological Society of America*, 97(3): 961–976.

Holzer, T. L., Bennett, M. J., Ponti, D. J., and Tinsley, J. C., III 1999. Liquefaction and soil failure during 1994 Northridge earthquake. *Journal of Geotechnical and Geoenvironmental Engineering*, 125(6): 438-452.

Idriss, I.M. & Boulanger, R.W. 2008. Soil liquefaction during earthquakes. Monograph MNO-12, Earthquake Engineering Research Institute, Oakland, CA, 261 pp.

Ishihara, K., and Koga, Y. (1981). "Case studies of liquefaction in the 1964 Niigata earthquake." *Soils and Foundations*, 21(3): 35-52.

Iwasaki, T., Tatsuoka, F., Tokida, K., & Yasuda, S. 1978. A practical method for assessing soil liquefaction potential based on case studies at various sites in Japan. *Proceedings, 2nd International Conference on Microzonation,* Nov 26-Dec 1, San Francisco, CA, USA.

Kayen, R. E., Mitchell, J. K., Seed, R. B., and Nishio, S. 1998. Soil liquefaction in the east bay during the earthquake. The Loma Prieta, California, Earthquake of October 17, 1989 – Liquefaction. Thomas L. Holzer, editor, USGS Professional Paper 1551-B, B61-B86.

Lee, D.H., Ku, C.S., and Juang, C.H. 2000. Preliminary investigation of soil liquefaction in the 1999 Chi-Chi, Taiwan, earthquake, *Proceedings, International Workshop on Annual Commemoration of Chi-Chi Earthquake, Vol. III – Geotechnical Aspect*, C.H. Loh and W.I. Liao, eds., National Center for Research on Earthquake Engineering, Taipei, Taiwan, pp. 140-151.

Maurer, B.W., Green, R.A., Cubrinovski, M., and Bradley, B.A. 2014. Evaluation of the liquefaction potential index for assessing liquefaction hazard in Christchurch, New Zealand. *Journal of Geotechnical and Geoenvironmental Engineering* 140(7): 04014032.

Maurer, B.W., Green, R.A., and Taylor, O.S. 2015a. Moving towards an improved index for assessing liquefaction hazard: lessons from historical data. *Soils and Foundations* 55(4), 778-787.

Maurer, B.W., Green, R.A., Cubrinovski, M., Bradley, B. 2015b. Fines-content effects on liquefaction hazard evaluation for infrastructure during the 2010-2011 Canterbury, New Zealand earthquake sequence. *Soil Dynamics and Earthquake Engineering*, 76, 58-68.

Maurer, B.W., Green, R.A., Cubrinovski, M., and Bradley, B. 2015c. Assessment of CPT-based methods for liquefaction evaluation in a liquefaction potential index framework. *Géotechnique* 65(5), 328-336.

Maurer, B.W. 2016. Moving towards an improved liquefaction hazard framework: lessons resulting from the 2010-2011 Canterbury, New Zealand, earthquake sequence. PhD Dissertation, Virginia Tech..

Mitchell, J. K., Lodge, A. L., Coutinho, R. Q., Kayen, R. E., Seed, R. B., Nishio, S., and Stokoe, K. H., II 1994. Insitu test results from four Loma Prieta earthquake liquefaction sites: SPT, CPT, DMT and shear wave velocity. Report No. UCB/EERC-94/04. Earthquake Engineering Research Center, UC Berkeley.

Moss, R. E. S., Seed, R. B., Kayen, R. E., Stewart, J. P., Youd, T. L., and Tokimatsu, K. 2003. Field case histories for CPT-based in situ liquefaction potential evaluation.

Geoengineering Research Rep. UCB/GE-2003/04.
Moss, R. E. S., Collins, B. D., and Whang, D. H. 2005. Retesting of liquefaction/nonliquefaction case histories in the imperial valley. *EQ Spectra*, 21(1): 179–196.
Moss, R.E.S, Seed, R.B., Kayen, R.E., Stewart, J.P., Der Kiureghian, A., & Cetin, K.O. 2006. CPT-based probabilistic and deterministic assessment of in situ seismic soil liquefaction potential. *J. Geotechnical and Geoenvironmental Eng,* 132(8), 1032-1051.
Moss, R. E. S., Kayen, R. E., Tong, L.-Y., Liu, S.-Y., Cai, G.-J., and Wu, J. 2009. Re-investigation of liquefaction and nonliquefaction case histories from the 1976 Tangshan earthquake. Rep. No. 209/102, Pacific Earthquake Engineering Research (PEER) Center, Berkeley, CA.
Moss, R. E. S., Kayen, R. E., Tong, L.-Y., Liu, S.-Y., Cai, G.-J., and Wu, J. 2011. Retesting of liquefaction and nonliquefaction case histories from the 1976 Tangshan earthquake. *Journal of Geotechnical and Geoenvironmental Engineering*, 137(4): 334-343.
NZGD 2016. New Zealand Geotechnical Database. <https://www.nzgd.org.nz/Default.aspx> Accessed 8/24/16. New Zealand Earthquake Commission (EQC).
Papathanassiou, G., Mantovani, A., Tarabusi, G., Rapti, D., and Caputo, R. 2015. Assessment of liquefaction potential for two liquefaction prone areas considering the May 20, 2012 Emilia (Italy) earthquake. *Engineering Geology*, 189:1-16.
Pass, D. G. 1994. Soil characterization of the deep accelerometer site at Treasure Island, San Francisco, California. MS thesis, University of New Hampshire.
PEER 2000a. Documenting Incidents of Ground Failure Resulting from the 1999, Kocaeli, Turkey Earthquake. http://peer.berkeley.edu/publications/turkey/adapazari/
PEER 2000b. Documentation of Soil Conditions at Liquefaction Sites from 1999 Chi-Chi, Taiwan Earthquake. http://peer.berkeley.edu/lifelines/research_projects/3A02/
Porter, K. 2016. A Beginner's Guide to Fragility, Vulnerability, and Risk. University of Colorado, 92 pp.
Quigley, M., Hughes, M.W., Bradley, B.A., van Ballegooy S., Reid, C., Morgenroth, J., Horton, T., Duffy, B., Pettinga, J. 2016. The 2010-2011 Canterbury earthquake sequence: Environmental effects, seismic triggering thresholds, geologic legacy. *Tectonophysics*, (672-673), 228-274.
Robertson, P.K. & Wride, C.E. 1998. Evaluating cyclic liquefaction potential using cone penetration test. *Canadian Geotechnical Journal*, 35(3), 442-459.
Seed, H.B. and Idriss, I.M. 1971. Simplified procedure for evaluating soil liquefaction potential. *Journal Soil Mechanics and Foundation Div*., 97(9): 1249-1273.
Seed, H. B., Tokimatsu, K., Harder, L. F. Jr., and Chung, R. 1984. The influence of SPT procedures in soil liquefaction resistance evaluations. Report No. UCB/EERC-84/15. Earthquake Engineering Research Center, University of California, Berkeley.
Servizio Geologico 2016. Database of the Emilia-Romagna Region: Geological, Seismic, and Soil Survey." http://ambiente.regione.emiliaromagna.it/geologia/cartografia/webgis-banchedati/ (Italian).
Shengcong, F. and Tatsuoka, F. 1984. Soil liquefaction during Haicheng and Tangshan earthquake in China; A review. *Soils and Foundations*, 24(4): 11-29.
Shibata, T., and Teparaska, W. 1988. Evaluation of Liquefaction Potential of Soils Using Cone Penetration Testing. *Soils and Foundations*, 28(2): 49-60.
Suzuki, Y., Tokimatsu, K., Moss, R. E. S., Seed, R. B., and Kayen, R. E. 2003. CPT-based liquefaction case histories from the 1995 Hyogoken-Nambu (Kobe) earthquake, Japan. Geotechnical Engineering Research Report No. UCB/GE-2003/03.
Tonkin + Taylor 2013. Liquefaction vulnerability study. T&T Ref: 52020.0200/v.1.0, prepared for New Zealand Earthquake Commission.
Toprak, S., and Holzer, T. L. (2003). "Liquefaction potential index: Field assessment." *Journal of Geotechnical and Geoenvironmental Engineering*, 129(4): 315-322.
Turner, B., Brandenberg, S., and Stewart, J. (2016). "Case Study of Parallel Bridges Affected by Liquefaction and Lateral Spreading." *Journal of Geotechnical and Geoenvironmental Engineering*, 142(7): 05016001.
Van Ballegooy, S., Malan, P., Lacrosse, V., Jacka, M.E., Cubrinovski, M., Bray, J.D., O'Rourke, T.D., Crawford, S.A., and Cowan, H. 2014a. Assessment of liquefaction-induced land damage for residential Christchurch. Earthquake Spectra, 30(1): 31-55.
Van Ballegooy, S., Cox, S.C., Thurlow, C., Rutter, H.K., Reynolds T., Harrington, G., Fraser, J., and Smith, T. 2014b. Median water table elevation in Christchurch and surrounding area after the 4 September 2010 Darfield earthquake: Ver 2. GNS Report 2014/18.
Van Ballegooy, S., Green, R.A., Lees, J., Wentz, F., and Maurer, B.W. 2015. Assessment of various CPT based liquefaction severity index frameworks relative to the Ishihara (1985) H_1-H_2 boundary curves. *Soil Dynamics and Earthquake Engineering,* 79, 347-364.
Youd, T. L., and Carter, B. L. 2005. Influence of soil softening and liquefaction on spectral acceleration. *Journal of Geotechnical and Geoenvironmental Engineering*, 131(7): 811-825.
Youd, T. L., DeDen, D. W., Bray, J. D., Sancio, R., Cetin, K. O., and Gerber, T. M. 2009. Zero displacement lateral spreads, 1999 Kocaeli, Turkey, earthquake. *Journal of Geotechnical & Geoenvironmental Engineering*, 135(1): 46-61.